Article

Ultra-robust Biochips with Metal-Organic Framework Coating for Point-of-Care Diagnosis

Congzhou Wang, Lu Wang, Sirimuvva Tadepalli, Jeremiah J. Morrissey, Evan D. Kharasch, Rajesh R. Naik, and Srikanth Singamaneni

ACS Sens., **Just Accepted Manuscript** • DOI: 10.1021/acssensors.7b00762 • Publication Date (Web): 16 Jan 2018

Ultra-robust Biochips with Metal-Organic Framework Coating for Point-of-Care Diagnosis

Congzhou Wang, Lu Wang, Sirimuvva Tadepalli, Jeremiah J. Morrissey, Evan D. Kharasch, Rajesh R. Naik, and Srikanth Singamaneni**

Dr. C. Wang, L. Wang, S. Tadepalli and Prof. S. Singamaneni
Department of Mechanical Engineering and Materials Science, Institute of Materials Science and Engineering, Washington University in St. Louis, Saint Louis, MO 63130, USA
E-mail: singamaneni@wustl.edu

Prof. J. J. Morrissey and Prof. E. D. Kharasch
Department of Anesthesiology, Washington University in St. Louis, St. Louis, MO, 63110, USA
Siteman Cancer Center, Washington University in St. Louis, St. Louis, MO, 63110, USA
The Center for Clinical Pharmacology, St. Louis College of Pharmacy and Washington University School of Medicine, St. Louis, MO, USA

Dr. R. R. Naik
711th Human Performance Wing, Air Force Research Laboratory, Wright-Patterson Air Force Base, Dayton, OH 45433
E-mail: rajesh.naik@us.af.mil

Abstract: Most biosensors relying on antibodies as recognition elements fail in harsh environment conditions such as elevated temperatures, organic solvents or proteases because of antibody denaturation, and require strict storage conditions with defined shelf-life, thus limiting their applications in point-of-care and resource-limited settings. Here, a metal-organic framework (MOF) encapsulation is utilized to preserve the biofunctionality of antibodies conjugated to nanotransducers. This study investigates several parameters of MOF coating (including growth time, surface morphology, thickness and precursor concentrations) that determine the preservation efficacy against different protein denaturing conditions in both dry and wet environments. A plasmonic biosensor based on gold nanorods as the nanotransducers is employed as a model biodiagnostic platform. The preservation efficacy attained through MOF encapsulation is compared to two other commonly employed materials (sucrose and silk fibroin). The results show that MOF coating outperforms sucrose and silk fibroin coatings under several harsh conditions including high temperature (80 °C), dimethylformamide and protease solution, owing to complete encapsulation, stability in wet environment and ease of removal at point-of-use by the MOF. We believe this study will broaden the applicability of this universal approach for preserving different types of on-chip biodiagnostic reagents and biosensors/bioassays, thus extending the benefits of advanced diagnostic technologies in resource-limited settings.

Keywords: *plasmonic biosensor, metal-organic framework, silk, sucrose, temperature, resource-limited settings, preservation*

Diagnostic technologies have developed tremendously over the past few decades.[1-2] However, most state-of-the-art technology platforms are centralized, expensive and require well-trained technicians with specialized facilities, which are inaccessible to most patients and clinicians in resource-limited settings, as well as those in low and middle-income countries.[3-4] Point-of-care (POC) testing allows patients and clinicians to make quick clinical decisions in a variety of settings such as clinical laboratories, doctors' offices, patients' home, disaster struck regions, battle fields and rural areas, by minimizing the turnaround time and cost to obtain a test result.[5-6] POC biosensors enable the rapid detection of clinically relevant biomarkers in biofluids (blood, urine, saliva, sweat, and tears) outside centralized laboratories, thus facilitating an earlier diagnosis and prompt treatment.[5] The basic elements of POC biosensors are similar to conventional laboratory instruments, consisting of a biorecognition element, transducer and readout modality. There have been extensive efforts on developing different types of transducers and readout devices for improving the sensitivity, accuracy and applicability of the biosensors for POC diagnosis.[7-11] Yet, an often-overlooked aspect is the limited shelf-life of the biosensors, which is highly dependent on the structural integrity and functionality of the biorecognition element.

The ability to recognize the "target" biomarker in a complex biofluid medium is viewed as the critical step in any diagnostic assay. One of the most common biorecognition elements employed in biodiagnostic devices are antibodies.[12] A typical example is lateral flow assays based on immobilized antibodies for pregnancy testing.[13] Unfortunately, as with most proteins, the antibodies are "fragile" in that they degrade and lose biofunctionality when subjected to various harsh conditions such as elevated temperatures, high humidity, organic solvents and proteolytic substances.[14-17] These conditions could be encountered during transport, handling and storage the biosensors in resource-limited settings where lack of facilities such as refrigeration/electricity, awareness of cautious handling, or availability of packaging/sealing methods, severely compromise the reliability of the bioanalytical results and hindering practical applications of the POC biosensors. To date, several approaches have been utilized to stabilize the biodiagnostic reagents including enzymes and antibodies either in solution or bound to solid surfaces. It is well accepted that dried reagents (*via*

freeze-drying or lyophilization) typically exhibit improved stability relative to those stored under wet conditions although temperature control for storage of dry reagents is still needed.[18-19] The addition of preservatives, sugar being the most common one, is another widely applied method to improve bioreagent stability and retention of activity, especially for chip-bound dry molecules.[6, 20] For instance, protein G beads dried with sucrose were shown to be stable for at least 1 month of storage at 45 °C.[21] This sugar-based stabilization is often attributed two mechanisms, namely, vitrification and water replacement. Vitrification occurs when the molecular mobility of the protein is restricted by the rigid sugar matrix, whereas stabilization by water replacement results from hydrogen bonds between protein and water being replaced by hydrogen bonds between sugar and protein during the drying process.[22-23] However, there is not a universal and robust approach for preserving on-chip antibodies in extremely harsh conditions that could be encountered in resource-limited settings. Such conditions may involve both dry and wet environments such as elevated temperatures, high humidity or aqueous solution, as well as organic solvents and proteolytic substances.

Metal-organic frameworks (MOFs), comprised of metal ions or clusters linked by organic ligands,[24-25] have shown promising applications in gas and energy storage,[26-27] drug delivery,[28] catalysis,[29-30] separation,[31-32] and chemical sensors.[33] Their attractive properties include large surface area, tunable porosity, organic functionality, stable shelf-life and excellent thermal stability.[34-37] Incorporation of biomolecules into these hybrid materials to form MOF biocomposites has opened up novel prospects in the utilization of MOFs.[38] Progress in the synthesis and application of MOF biocomposites has been recently reviewed by Falcaro and co-authors.[39] Among the synthesis methods, encapsulating biomolecules *via* a spontaneous process analogous to natural biomineralization offers several unique advantages: i) the synthesis simply involves incubating biomolecules with MOF precursors in mild aqueous solution, which is critical to maintain biomolecular activity; ii) it does not require a MOF with pores larger than the biomolecule, which not only prevents leaching but also takes advantage of the small pore size of MOFs for various applications; iii) since biomolecules can promote MOF nucleation and crystallization, this approach is universal for all different types of biomolecules. So far, this approach is mainly used to encapsulate free

enzymes in solution for biocatalysis.[40-43] Such encapsulation confines the structural change of enzymes and inhibits the loss of bioactivity. In this case, the MOF pore size should be significantly smaller than protein size to prevent protein leakage and restrict protein mobility, while the pore size of MOF should be large enough to allow substrate and product molecules to diffuse in and out of the MOF for efficient biocatalytic reaction.[44] In addition to these applications, we recently demonstrated that a zeolitic imidazolate framework-8 (ZIF-8) film can be grown on antibody-conjugated gold nanorods, and such coatings are highly effective in preserving the biorecognition capabilities of these plasmonic biosensors that are exposed to ambient and elevated temperatures.[45] However, considering complicated and unexpected environment conditions in resource-limited settings, elevated temperature is not the only factor that could compromise the reliability and applicability of these POC biosensors.

Herein, we evaluated the preservation efficacy of the MOF-based approach against a variety of harsh environmental conditions (including elevated temperature, organic solvent and proteolytic degradation) that would lead to denaturation of antibodies and loss of biofunctionality of the biochips (Figure 1). Using gold nanorods (AuNRs) as nanotransducers, a plasmonic nanobiosensor based on refractive index sensitivity of localized surface plasmon resonance (LSPR) is used as a model POC biosensor. Plasmonic biosensor fabrication steps (including conjugation of antibody to the surface of AuNRs, growth and removal of MOF film, as well as bioanalyte detection) can be monitored by following the LSPR wavelength shift of the AuNRs. Several parameters related to ZIF-8 film growth (such as growth time, surface morphology, thickness and precursor concentrations) are examined and optimized to obtain highest biopreservation within both dry and wet environments. Finally, we compared the ZIF-8 coating with sucrose and silk coatings, in terms of their biopreservation performances. Overall, these detailed studies will contribute toward further understanding and practical applications of MOF-based biopreservation approach. We believe this study will also broaden the applicability of this universal approach for preserving different types of on-chip biodiagnostic reagents and biosensors/bioassays for POC diagnosis in resource-limited settings with unexpected harsh

environmental conditions.

Results and discussion

Fabrication and test of antibody-based plasmonic biochip

Gold nanorods (AuNRs) are considered to be an attractive choice as plasmonic nanotransducers for label-free biosensing owing to their large refractive index sensitivity and facile tunability of the LSPR wavelength.[46] Using a seed-mediated approach,[47-49] we synthesized AuNRs with a length of 55 ± 2 nm and a diameter of 14 ± 1 nm (Figure 2A). Rabbit IgG (henceforth IgG) was employed as the model biorecognition element to capture the model target bioanalyte, goat anti-Rabbit IgG (anti-IgG). As described earlier, conjugation of AuNRs with the antibodies follows two steps.[50] The IgG molecules were initially modified with a bifunctional polyethylene glycol chain (COOH-PEG-SH) using a carbodiimide coupling chemistry. IgG-PEG-SH was then covalently attached onto the AuNRs surface through a gold-thiol linkage. The flexible PEG chain not only increases the accessibility of IgG to target bioanalyte, but also serves as an anti-fouling layer around the AuNRs surface to minimize the non-specific binding of interfering proteins.[51] The conjugation of IgG onto AuNRs in solution led to a red shift of 9.2 nm in the longitudinal LSPR wavelength due to the increase in the refractive index of the medium surrounding the AuNRs (Figure 2B). Dynamic light scattering showed increased hydrodynamic size (~8 nm increase) of AuNR-IgG compared to bare AuNR, further confirming the conjugation of IgG onto AuNRs (Figure S1). Subsequently, AuNR-IgG conjugates were immobilized onto glass substrates by incubating the (3-mercaptopropyl)-triethoxy-silane modified glass substrates with the nanobioconjugate solution followed by thoroughly rinsing with ultrapure water to remove any weakly bound AuNR-IgG conjugates. To test the sensing capability of the plasmonic biochip, the biochips were exposed to a series of concentrations of anti-IgG. A monotonic increase in the red shift of LSPR wavelength was noted with an increase in the anti-IgG concentration (Figure 2C). Since LSPR wavelength exhibited maximal red shift (~34.5 nm) at the highest concentration of anti-IgG (24 μg/ml) (Figure 2D), this concentration was employed to quantify

the biorecognition ability of the biochip and evaluate the preservation efficacy of MOF approach against different harsh environmental conditions in subsequent experiments. On the other hand, significantly smaller red shifts of ~2 nm were observed upon exposure to human serum albumin (HSA, 240 μg/mL) or hemoglobin (Hb, 240 μg/mL), indicating the excellent specificity of AuNR-IgG conjugates (Figure S2). It should be noted that conjugation of IgG with PEG-thiol is necessary to maintain the recognition ability of IgG, as demonstrated by a control experiment wherein AuNRs with physically-absorbed IgG only showed ~14 nm red shift at the highest concentration of anti-IgG (Figure S3).

Formation and characterization of ZIF-8 coating on biochip

Previous reports have shown that a MOF coating can spontaneously form on various biological surfaces such as surface immobilized proteins, virus and bacterial surfaces, suggesting that the biomacromolecules can act as preferential MOF nucleation sites.[52-54] Here, we hypothesize that the antibodies immobilized on the plasmonic nanotransducers can induce MOF formation around the biofunctionalized nanostructures. Formation of MOF crystals tightly confines the antibodies and resists structural and functional changes in antibodies, thus increasing the biochip stability and shelf-life. To form the MOF encapsulation, the biochips with the AuNR-IgG conjugates were immersed into ZIF-8 precursor solution (a mixture of 2-methylimidazole and zinc acetate with a molar ratio of 4:1) to grow the ZIF-8 nanocrystals *in situ*. After 3 h incubation, the LSPR wavelength displayed a ~50 nm red shift, suggesting the formation of a ZIF-8 coating on top of the AuNR-IgG conjugates (Figure 3A and 3B, from step1 to step2). The atomic force microscopy (AFM) images also displayed the distinct morphology change from uniformly distributed nanobioconjugates on glass substrate to homogeneous ZIF-8 nanocrystals covering the underneath nanobioconjugates (Figure 3C and 3D). Besides the facile formation, the ease of removal of the nanocrystals is equally important to ensure the on-demand use of the biochip after storage for a desired duration under available environmental conditions. The ZIF-8 protective coating can be easily removed by rinsing the biochip with water at pH 6 due to the loss of the coordination between the zinc ions and imidazolate under a slightly acidic environment.[55-56] The complete removal of the ZIF-8 coating was evidenced by a ~50 nm

blue shift (Figure 3A and 3B, from step 2 to step 3) in the LSPR wavelength and further confirmed by the AFM image (Figure 3E). Subsequently, the restored biochip exhibited a red shift of ~30 nm when exposed to 24 μg/mL of anti-IgG (Figure 3A and 3B, from step 3 to step 4). As reported previously,[45, 57] we evaluate the preservation efficacy of MOF approach against different harsh conditions using the percentage of retained recognition capability (%), which is calculated as the percentage of the red shift upon detecting anti-IgG using a restored chip after storage under different conditions compared to the red shift detected with the same batch of freshly fabricated biochips (reference biochip tested instantly without coating process). For instance, a red shift of ~30 nm after storage compared to the red shift of ~34.5 nm obtained from the reference biochip in the same batch corresponds to a retained recognition capability of ~87%. This method provides a quantitative and simple means to evaluate the recognition capability of biochips and efficacy of MOF preservation.

Raman spectroscopy and X-ray diffraction (XRD) were performed to ascertain that ZIF-8 crystals were formed on the biochip surface. The Raman scattering spectrum of pristine nanoconjugates depicted amide I and amide III bands of the protein, as well as a peak at ~1450 cm^{-1} corresponding to CH_2 bending mode of capping reagent (cetyltrimethylammonium bromide (CTAB)) of AuNRs.[58] After ZIF-8 coating, characteristic peaks of 2-methylimidazole were observed at 1142, 1178, 1459 and 1500 cm^{-1} corresponding to C−N stretching, C−N stretching plus N−H wagging, C−H wagging and C−N stretching plus N-H wagging, respectively (Figure 3F).[59-60] XRD measurements also confirmed the formation of ZIF-8 crystals on the biochip surface (Figure 3G). The related peak positions in XRD patterns were consistent with the typical structure of pure ZIF-8.[61-62]

ZIF-8 coating against elevated temperatures

In our previous study, we demonstrated that a plasmonic biochip with the ZIF-8 coating retained over 80% of recognition capability when stored at room temperature for one week.[45] This preservation efficacy meets and exceeds the need for short-term use of the biochips within resource-limited settings. However, long-term temperature stability of the biochips, which is important for patient surveillance, especially in remote areas without a logistic

network, cold chain storage and clinical laboratories, is still unknown. To increase the shelf-life of the biochip, we set out to optimize the MOF growth parameters and evaluate the preservation efficacy of the MOF coatings against high temperatures (at 40, 60 and 80 °C). These temperatures serve as surrogates for long-term storage at room temperature.

The plasmonic biochips were first coated with ZIF-8 crystals by incubating the biochips in ZIF-8 precursors for 3 h. Then the biochips with and without the ZIF-8 coating were stored at 40, 60 and 80 °C for 1 day. The results showed that the ZIF-8 film coated biochip retained over 80% at both 40 and 60 °C and ~50% of recognition capability at 80 °C (Figure 4A). In contrast, the biochips without ZIF-8 coating lost over 70% of recognition capability across these three temperatures. This rather poor preservation efficacy at 80 °C may be due to the incomplete and imperfect encapsulation of antibodies. We posit that increasing the ZIF-8 film growth time would improve MOF encapsulation of the antibodies. To test this hypothesis, we increased the ZIF-8 film growth time from 3 h to 24 h and found that 24 h incubation offered the highest preservation efficacy, particularly at 80 °C, compared to both 3 and 12 h film growth. Time-lapse AFM imaging was employed to monitor the growth of ZIF-8 film on the biochip surface. Figure 4C-E clearly indicated the increase in the size of ZIF-8 crystals with the increase of growth time. The AFM scratch tests revealed that the thickness of the ZIF-8 film also increased with increase in the film growth time (Figure 4B and Figure S4), which also led to the increased LSPR red shifts (from ~50 nm for 3h to ~55 nm for 24 h). At 80°C, the retained activity increased with an increase in the film thickness. Such correlation was not observed at lower storage temperatures (Figure S5). This is probably because the mobility of protein chains at 40 and 60°C is not as high as protein chains at 80°C and a relatively thin film is sufficient to resist protein mobility at these temperatures. In the case of 80°C, the proteins lose their secondary structure rapidly and need to be tightly confined within a thicker film. Furthermore, the XRD pattern showed an increase in the crystallinity (demonstrated by the increase of peak intensity)[40] with the increase of film growth time (Figure S6). In order to probe the temperature upper limit that the biochips can withstand, we also attempted to preserve the biochips at 100 and 120 °C. However, the AuNRs themselves were not stable at these temperatures, as demonstrated by ~15-20 nm

blue shift in the LSPR wavelength associated with altered morphology shown in AFM image (Figure S7). This finding is in agreement with a previous study that showed blue shift in LSPR wavelength of AuNRs under 100-250 °C due to the surface melting of AuNRs.[63] Overall, these results suggest that extending the ZIF-8 growth time can minimize the defects on ZIF-8 film formation and improve the encapsulation, thereby conferring improved temperature stability to the biochips. With the optimized ZIF-8 coating, we further extended the incubation time and the results showed that ZIF-8 coated biochips retained over 70% recognition ability after one week incubation at 80°C. This retained recognition ability is comparable with that of the refrigerated biochips (stored at 4°C) (Figure S8).

ZIF-8 coating against organic solvent and protease

In real-world applications, elevated temperature is not the only detrimental condition that compromises the stability of biochips. Considering the unexpected environmental conditions that may be encountered during transport, handling and storage of biochips, it is important to assess the preservation efficacy of ZIF-8 coating within wet environments such as organic solvents and aqueous solution containing proteolytic substances. Toward this end, the biochips with (24 h growth time) and without ZIF-8 coating were exposed to dimethylformamide (DMF) and separately to a protease (protease from *Streptomyces griseus*, dissolved in pH 7.4 phosphate-buffered saline at 37 °C). Polar solvents (*e.g.* DMF, dimethylsulfoxide, formamide) can drive water molecules away from the protein surface and compete for hydrogen bonds existing between the proteins and water molecules, which often denatures the protein and results in the loss of specific binding activity.[64-65] Proteases represent another type of protein degrading reagents through cleaving the peptide bonds of proteins.[66] After 1 h of immersion in DMF or protease solution, the ZIF-8 coating failed to preserve the recognition capability of the biochips in both cases (Figure 5A, blue bars). It is noteworthy that the LSPR wavelength of AuNR-antibody conjugates coated with ZIF-8 exhibited a ~40 nm blue shift after exposure to DMF or protease solution (Figure 5B and C, black plots). Moreover, the AFM images revealed the exposed AuNR-IgG conjugates due to the disintegration of ZIF-8 film (Figure 5D). These observations indicate the poor stability of the ZIF-8 coating within these two media, leading to the disintegration of the ZIF-8 coating

and subsequent loss of the biorecognition of the antibodies. Similar phenomenon was observed by Gassensmith and co-workers, where they found that the ZIF-8 film (with a same (4:1) molar ratio of 2-methylimidazole and zinc acetate) was unstable after the sample was removed from mother liquor solution containing the ZIF-8 precursors.[53] Based on this finding, we adjusted the molar ratio of 2-methylimidazole and zinc acetate to 40:1, and observed ~65 nm red shift in the LSPR wavelength (higher than ~55 nm red shift using 4:1 ratio, Figure 5B and 5C) due to the formation of thicker film (~28 nm thickness measured by AFM scratch) (Figure S4D). More importantly, such coatings did not disintegrate after immersing the biochips into DMF or protease solution (Figure 5E and 5F), and thereby the preservation efficacy in both cases was greatly improved (Figure 5A, red bars). It should be noted that the preservation mechanism of ZIF-8 coating against DMF or protease exposure is different, considering that the DMF can penetrate and move through the ZIF-8 pores[62], while the protease is too large to enter the pores.[41] Hence, ZIF-8 encapsulation confines the structure and functional degradation of antibody due to the presence of DMF, whereas protease is shielded by the ZIF-8 coating.

Comparison among ZIF-8, sucrose and silk coatings

Finally, we sought to compare the preservation efficacy of ZIF-8, sucrose and silk fibroin coatings. Silk fibroin was reconstituted from Bombyx mori silkworm cocoon following a reported protocol.[67] As described above, sugars such as sucrose and trehalose have been frequently used as stabilizers in the dry preservation of biomolecules.[68-70] In our previous study, silk fibroin showed excellent ability as a coating material for preservation of antibodies against temperature degradation.[57] Herein, the preservation efficacy of the three materials against elevated temperature, organic solvent (DMF) or protease were systematically investigated and compared. Silk fibroin and sucrose films were spin-coated onto biochip surfaces. AFM scratch measurements showed the complete coverage of the biochip surface with ~100 nm thick silk and sucrose films (Figure S9). Figure 6A summarizes the preservation efficacy of the three materials at 80 °C. Sucrose-coated biochips retained ~20% lower recognition capability compared to ZIF-8 coated biochip probably due to the inferior encapsulation provided by the sucrose. The silk-coated biochip completely lost the

recognition capability since the silk film incubated at 80 °C for 1 day could not be removed by water rinsing (indicated by the LSPR wavelength shift, Figure 6D) and thereby the antibodies could not be exposed for analyte detection. The elevated temperature here induced the initial soluble silk I to transit to insoluble silk II state, leading to incomplete removal of silk film and inaccessibility of the antibodies (buried under silk film) to the analytes.[71] Hence, silk films are unsuitable for preservation at high temperatures or long storage times. Even in the case of DMF exposure (Figure 6B), ZIF-8 coated biochip retained the highest recognition capability, whereas sucrose did not exhibit significant preservation efficacy (compared to the control) due to the dissolution of sucrose in DMF,[72] evidenced by ~40 nm blue shift of LSPR wavelength after the biochip was removed from the solvent (Figure 6E). Similar to elevated temperatures, silk I was converted to insoluble silk II in DMF, resulting in the complete loss of recognition capability. Figure 6C reveals the preservation efficacy of the three materials against exposure to proteolytic conditions. In contrast to ZIF-8, both silk and sucrose coatings were dissolved in protease solution, leading to minimal preservation (Figure 6F). The silk film here can be completely dissolved and removed by aqueous solution, suggesting the predominant silk I structure in the film. Although it has been reported that silk II is highly resistant to protease attack,[73-74] silk II cannot be employed as a protective coating due to the difficulties (insoluble in water) associated with removing it, which is necessary for biochip restoration before use. Overall, sucrose and silk coatings did not perform as well as the MOF either because of the dissolution of the films in wet environment or incomplete removal of film during restoration. The ZIF-8 coating exhibited the best preservation efficacy against all three antibody denaturing factors including elevated temperature, DMF and proteolytic degradation.

Conclusion

In summary, we presented a MOF (ZIF-8)-based approach for preserving the biorecognition capability of antibodies on biochip surface by forming a protective coating on the top of the antibodies. The ultra-robust biochips with ZIF-8 protective coatings are able to withstand harsh environmental conditions (including elevated temperatures, an organic solvent and a

proteolytic substance) that would otherwise lead to denaturation of antibodies and loss of biofunctionality of the biochips. The ZIF-8 protective coating greatly improves the reliability and applicability of the biochips for deployment in resource-limited settings, as well as low and middle-income countries. The ZIF-8 coated biochips retained over 80% of recognition capability after one day of incubation at temperatures up to 80 °C, which serves as a surrogate for long-term storage at room temperature. The preservation efficacy at elevated temperatures can be improved *via* increasing the ZIF-8 film growth time and thickness, underscoring the importance of complete encapsulation of antibodies. Optimization of the precursor concentration resulted in ZIF-8 coatings that are stable in a wet environment, thus providing excellent preservation against organic solvent and protease solution. ZIF-8 coating exhibited superior preservation efficacy compared to other preservative coatings such as silk and sucrose owing to its stability in a wet environment and ease of removal before use. Overall, we believe the detailed studies in this work establish the MOF-based biopreservation of immobilized biomolecules that are common in a number of applications. This universal approach is expected to preserve different types of on-chip biodiagnostic reagents and biosensors/bioassays for POC diagnosis in resource-limited settings with harsh environmental conditions.

Supporting Information

Experimental details, DLS data of AuNR and AuNR-IgG, study of biochip specificity, AFM images of ZIF-8 film scratch experiments, correlation between the thickness of ZIF-8 film and retained activity of biochips, XRD spectra of ZIF-8-IgG, AFM images and LSPR spectra of AuNR-IgG before and after incubation at 120 °C, biochip stability within one week at different temperatures and AFM images of silk and sucrose film scratch experiments.

This material is available free of charge via the Internet at http://pubs.acs.org.

Acknowledgements

We acknowledge support from Air Force Office of Scientific Research (FA9550-15-1-0228 and 12RX11COR), AFRL/711 HPW and National Institutes of Health (R21DK100759 and R01CA141521). The authors thank the Nano Research Facility (NRF) at Washington University for providing access to electron microscopy facilities.

Figures

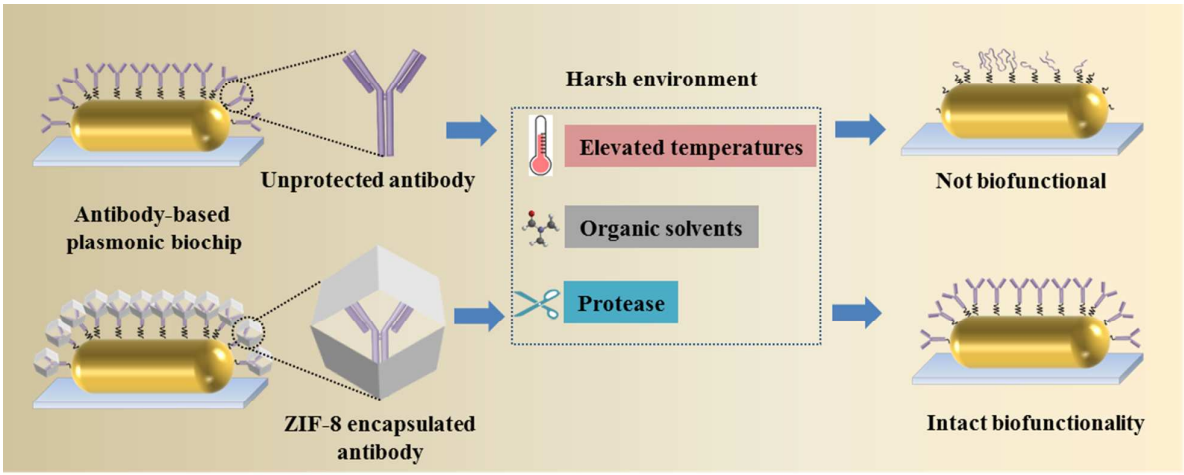

Figure 1. Schematic illustration depicting that ZIF-8 encapsulated antibody maintains biofunctionality when subjected to harsh environmental conditions, greatly improving the reliability and applicability of biochips in resource-limited settings.

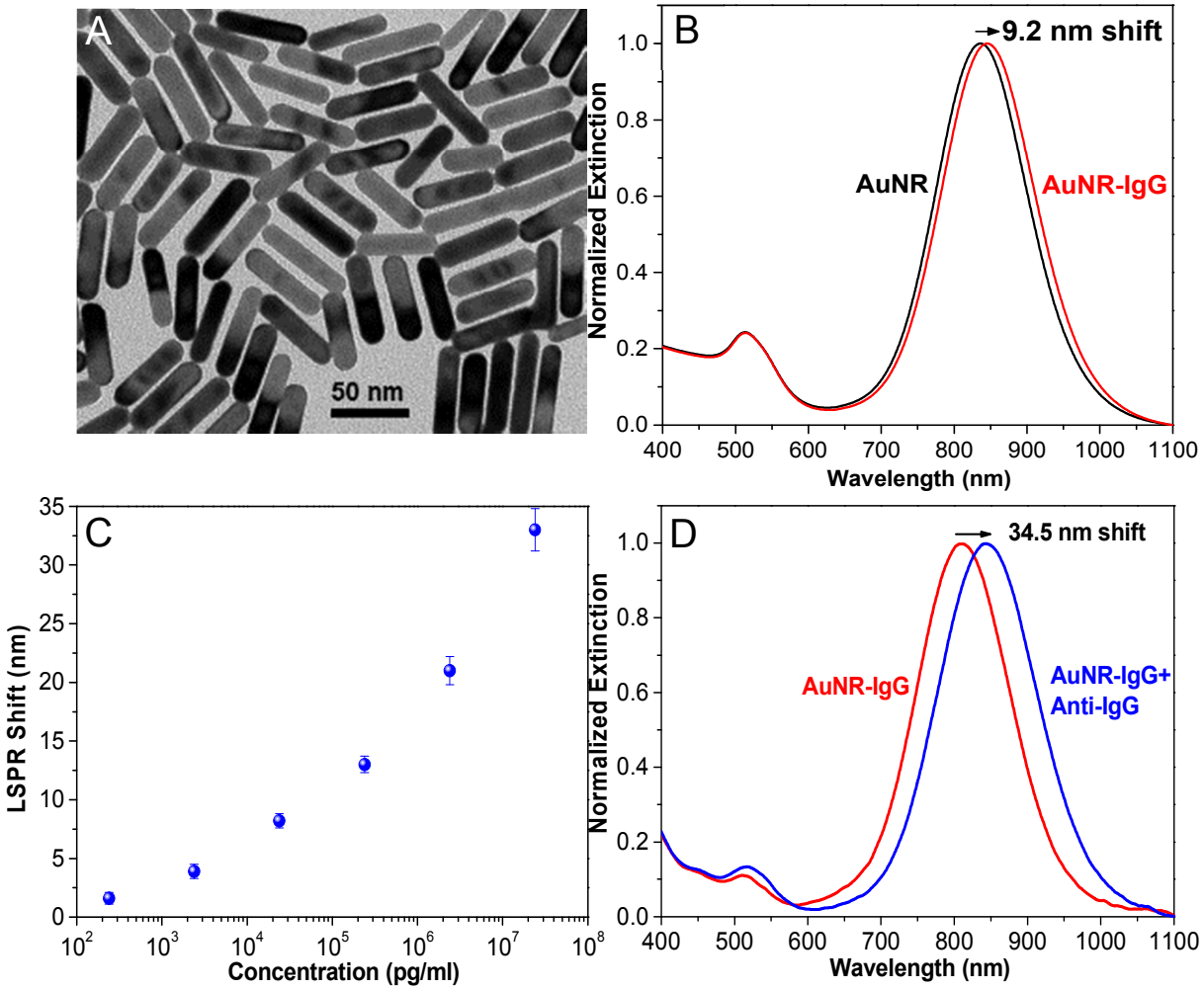

Figure 2. (A) TEM image of AuNRs used as nanotransducers for plasmonic biochips. The dimension of the AuNRs is 55×14 nm. (B) Extinction spectra showing the LSPR longitudinal wavelength shifts by 9.2 nm after conjugation of AuNRs with antibody (IgG) in solution. C) Plot showing the sensing ability of AuNR-IgG conjugates on glass substrate when detecting a series of concentrations of analyte (anti-IgG). Error bars represent standard deviations from three independent samples. (D) Extinction spectra of AuNR-IgG conjugates on the glass substrate before (red) and after binding with 24 μg/ml of anti-IgG (blue). The λ red shifts by 34.5 nm.

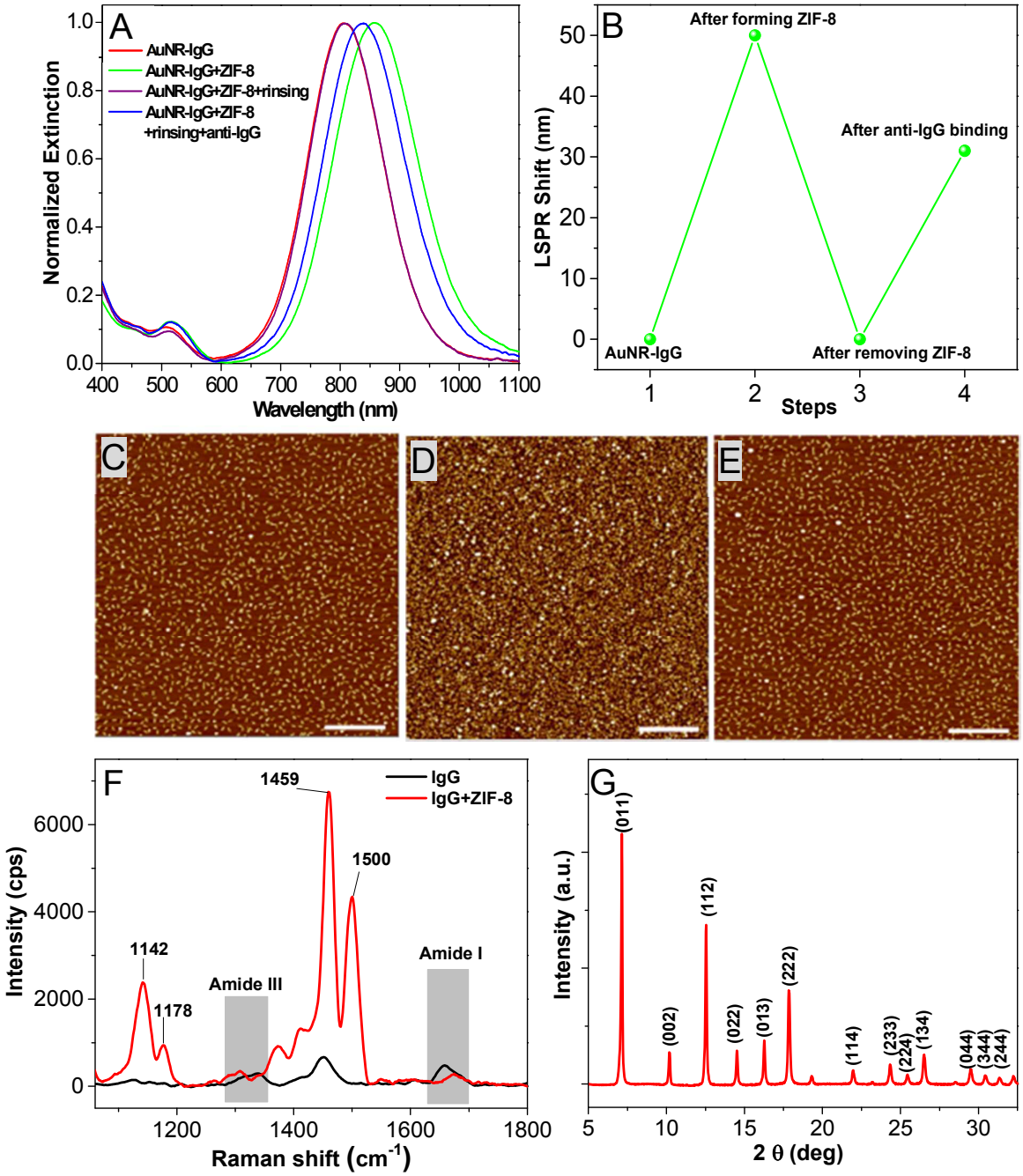

Figure 3. (A) Extinction spectra of AuNR-IgG conjugates on the glass substrate before (red) and after ZIF-8 coating (green), after removing ZIF-8 coating (purple) and after binding with 24 μg/ml of anti-IgG (blue). (B) LSPR wavelength shift corresponding to each step in (A). (C) AFM image showing uniformly adsorbed AuNR-IgG conjugates on glass substrate before ZIF-8 coating. (D) AFM image

showing ZIF-8 coating formed on the top of AuNR-IgG conjugates. (E) AFM image showing rinsing with pH 6 water could completely remove ZIF-8 coating and expose the underneath AuNR-IgG conjugates. (F) Raman spectra of AuNR-IgG before (black) and after ZIF-8 coating (red). (G) XRD spectrum of ZIF-8 with encapsulated IgG. Scale bars: 1 μm.

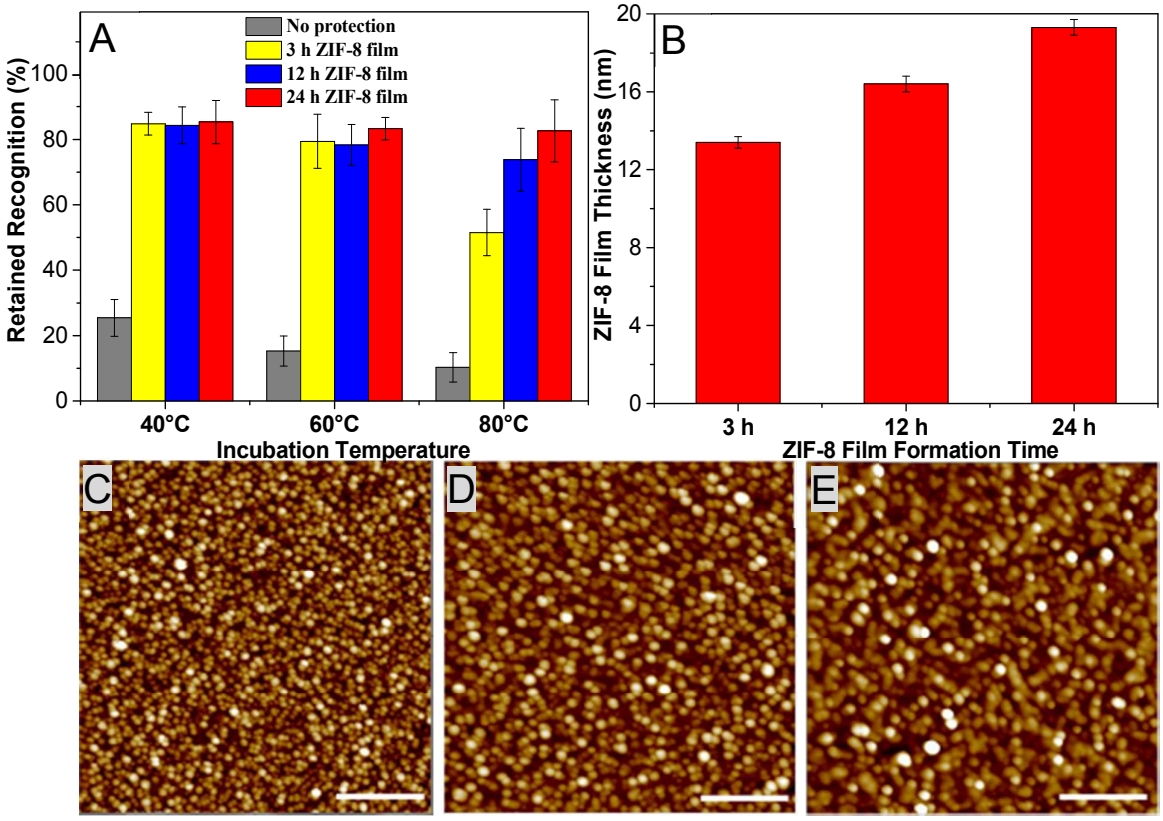

Figure 4. (A) Retained recognition capability of ZIF-8-coated biochips with different ZIF-8 film growth time stored at 40, 60 and 80 °C for 1 day. (B) ZIF-8 film thickness after different growth time measured by AFM scratch experiments. AFM images of ZIF-8 coating on the biochip after (C) 3 h growth; (D) 12 h growth; and (E) 24 h growth. Scale bars: 500 nm. Error bars represent standard deviations from three independent samples.

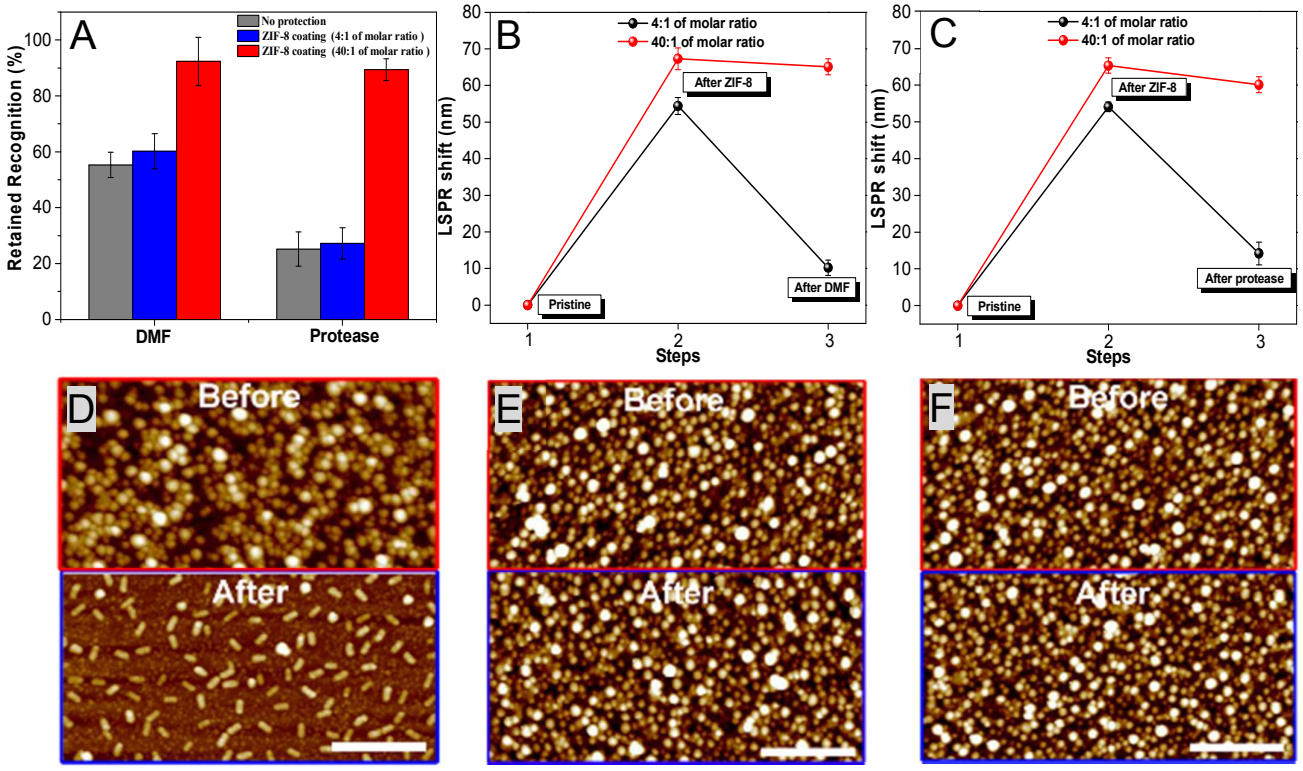

Figure 5. (A) Retained recognition capability of ZIF-8-coated biochips with different molar ratio of ZIF-8 film precursors after stored in DMF and protease solution for 1 h. (B) LSPR wavelength shift after coating the biochips with ZIF-8 using different molar ratio of precursors and after pulling the biochips from DMF. (C) LSPR wavelength shift after coating the biochips with ZIF-8 using different molar ratio of precursors and after pulling the biochips from protease solution. Error bars represent standard deviations from three independent samples. (D) AFM images of ZIF-8 film (4:1 molar ratio) before and after immersion into DMF. (E) AFM images of ZIF-8 film (40:1 molar ratio) before and after immersion into DMF. (F) AFM images of ZIF-8 film (40:1 molar ratio) before and after immersion into protease solution. Scale bars: 500 nm.

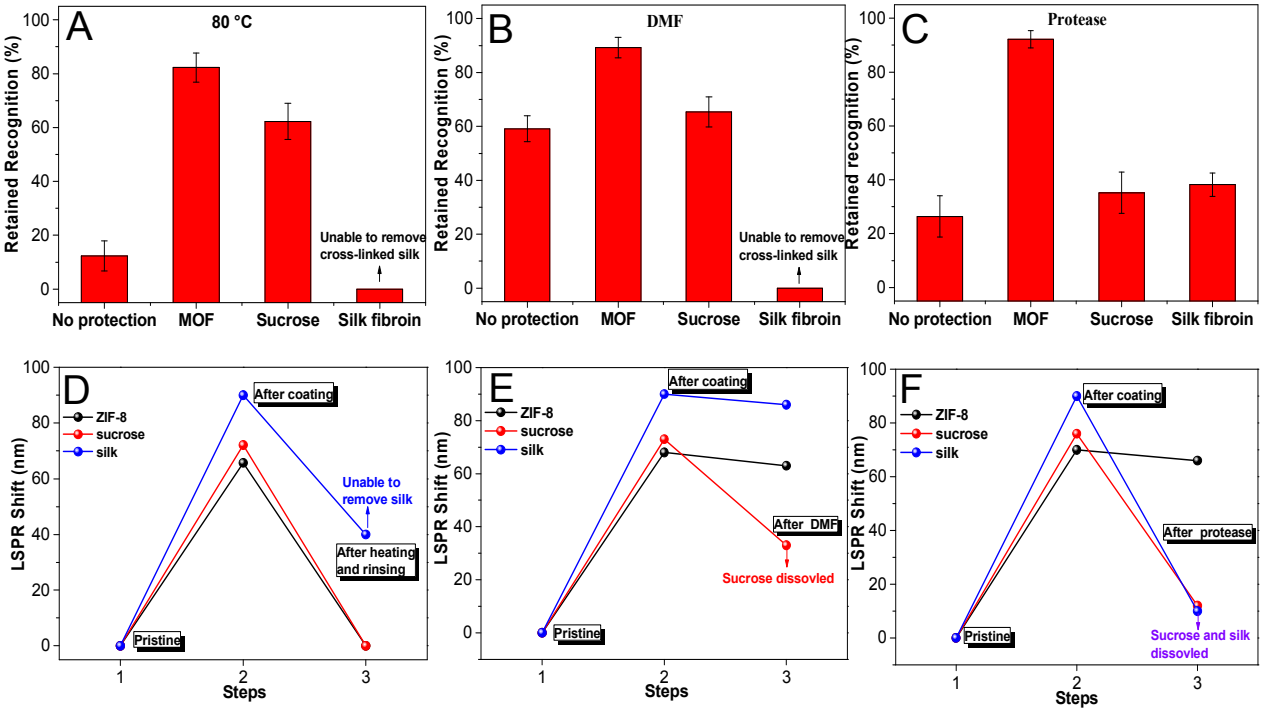

Figure 6. (A) Comparison of preservation efficacy against 80 °C among ZIF-8, sucrose and silk. (B) Comparison of preservation efficacy against DMF among ZIF-8, sucrose and silk. (C) Comparison of preservation efficacy against protease solution among ZIF-8, sucrose and silk. (D) LSPR wavelength shift after coating the biochips with three different materials and LSPR wavelength shift after rinsing the films after incubation of the biochips at 80 °C for 1 day. (E) LSPR wavelength shift after coating the biochips with three different materials and LSPR wavelength shift after pulling the biochips from DMF. (F) LSPR wavelength shift after coating the biochips with three different materials and LSPR wavelength shift after pulling the biochips from protease solution. Error bars represent standard deviations from three independent samples.

References

1. Chin, C. D.; Laksanasopin, T.; Cheung, Y. K.; Steinmiller, D.; Linder, V.; Parsa, H.; Wang, J.; Moore, H.; Rouse, R.; Umviligihozo, G.; Karita, E.; Mwambarangwe, L.; Braunstein, S. L.; van de Wijgert, J.; Sahabo, R.; Justman, J. E.; El-Sadr, W.; Sia, S. K., Microfluidics-based diagnostics of infectious diseases in the developing world. *Nat. Med.* **2011,** *17* (8), 1015-1019.

2. Drain, P. K.; Hyle, E. P.; Noubary, F.; Freedberg, K. A.; Wilson, D.; Bishai, W. R.; Rodriguez, W.; Bassett, I. V., Diagnostic point-of-care tests in resource-limited settings. *Lancet Infect. Dis.* **2014,** *14* (3), 239-249.

3. Mabey, D.; Peeling, R. W.; Ustianowski, A.; Perkins, M. D., Diagnostics for the developing world. *Nat. Rev. Microbiol.* **2004,** *2* (3), 231-240.

4. Peeling, R. W.; Mabey, D., Point-of-care tests for diagnosing infections in the developing world. *Clin. Microbiol. Infect.* **2010,** *16* (8), 1062-1069.

5. Soper, S. A.; Brown, K.; Ellington, A.; Frazier, B.; Garcia-Manero, G.; Gau, V.; Gutman, S. I.; Hayes, D. F.; Korte, B.; Landers, J. L.; Larson, D.; Ligler, F.; Majumdar, A.; Mascini, M.; Nolte, D.; Rosenzweig, Z.; Wang, J.; Wilson, D., Point-of-care biosensor systems for cancer diagnostics/prognostics. *Biosens. Bioelectron.* **2006,** *21* (10), 1932-1942.

6. Gubala, V.; Harris, L. F.; Ricco, A. J.; Tan, M. X.; Williams, D. E., Point of Care Diagnostics: Status and Future. *Anal. Chem.* **2012,** *84* (2), 487-515.

7. Inan, H.; Poyraz, M.; Inci, F.; Lifson, M. A.; Baday, M.; Cunningham, B. T.; Demirci, U., Photonic crystals: emerging biosensors and their promise for point-of-care applications. *Chem. Soc. Rev.* **2017,** *46* (2), 366-388.

8. Wang, J., Electrochemical biosensors: towards point-of-care cancer diagnostics. *Biosens. Bioelectron.* **2006,** *21* (10), 1887-1892.

9. Tokel, O.; Inci, F.; Demirci, U., Advances in plasmonic technologies for point of care applications. *Chem. Rev.* **2014,** *114* (11), 5728-5752.

10. Yetisen, A. K.; Akram, M. S.; Lowe, C. R., Paper-based microfluidic point-of-care diagnostic devices. *Lab on a Chip* **2013,** *13* (12), 2210-2251.

11. Luppa, P. B.; Müller, C.; Schlichtiger, A.; Schlebusch, H., Point-of-care testing (POCT): Current techniques and future perspectives. *Trends Anal. Chem.* **2011,** *30* (6), 887-898.

12. Chambers, R. S.; Johnston, S. A., High-level generation of polyclonal antibodies by genetic immunization. *Nat. Biotechnol.* **2003,** *21* (9), 1088-1092.

13. Posthuma-Trumpie, G. A.; Korf, J.; van Amerongen, A., Lateral flow (immuno) assay: its strengths, weaknesses, opportunities and threats. A literature survey. *Anal. Bioanal. Chem.* **2009,** *393* (2), 569-582.

14. Vermeer, A. W.; Norde, W., The thermal stability of immunoglobulin: unfolding and aggregation of a multi-domain protein. *Biophys. J.* **2000,** *78* (1), 394-404.

15. Pace, C. N.; Treviño, S.; Prabhakaran, E.; Scholtz, J. M., Protein structure, stability and solubility in water and other solvents. *Phil. Trans. R. Soc. B* **2004,** *359* (1448), 1225-1235.

16. Turk, B. E.; Huang, L. L.; Piro, E. T.; Cantley, L. C., Determination of protease cleavage site motifs using mixture-based oriented peptide libraries. *Nat. Biotech.* **2001,** *19* (7), 661-667.

17. Brandts, J. F.; Hunt, L., Thermodynamics of protein denaturation. III. Denaturation of ribonuclease in water and in aqueous urea and aqueous ethanol mixtures. *J. Am. Chem. Soc.* **1967,** *89* (19), 4826-4838.

18. Chin, C. D.; Linder, V.; Sia, S. K., Lab-on-a-chip devices for global health: Past studies and future opportunities. *Lab on a Chip* **2007,** *7* (1), 41-57.

19. Yager, P.; Edwards, T.; Fu, E.; Helton, K.; Nelson, K.; Tam, M. R.; Weigl, B. H., Microfluidic diagnostic technologies for global public health. *Nature* **2006,** *442* (7101), 412-418.

20. Crowe, J. H.; Carpenter, J. F.; Crowe, L. M., The role of vitrification in anhydrobiosis. *Annu. Rev. Physiol.* **1998,** *60*, 73-103.

21. McKenzie, K. G.; Lafleur, L. K.; Lutz, B. R.; Yager, P., Rapid protein depletion from complex samples using a bead-based microfluidic device for the point of care. *Lab on a Chip* **2009,** *9* (24), 3543-3548.

22. Grasmeijer, N.; Stankovic, M.; de Waard, H.; Frijlink, H. W.; Hinrichs, W. L. J., Unraveling protein stabilization mechanisms: Vitrification and water replacement in a glass transition temperature controlled system. *Biochimica et Biophysica Acta (BBA) - Proteins and Proteomics* **2013,** *1834* (4), 763-769.

23. Malsam, J.; Aksan, A., Hydrogen Bonding and Kinetic/Thermodynamic Transitions of Aqueous Trehalose Solutions at Cryogenic Temperatures. *The Journal of Physical Chemistry B* **2009,** *113* (19), 6792-6799.

24. Yaghi, O. M.; O'Keeffe, M.; Ockwig, N. W.; Chae, H. K.; Eddaoudi, M.; Kim, J., Reticular synthesis and the design of new materials. *Nature* **2003,** *423* (6941), 705-714.

25. Patterson, J. P.; Abellan, P.; Denny, M. S.; Park, C.; Browning, N. D.; Cohen, S. M.; Evans, J. E.; Gianneschi, N. C., Observing the Growth of Metal-Organic Frameworks by in Situ Liquid Cell Transmission Electron Microscopy. *J. Am. Chem. Soc.* **2015,** *137* (23), 7322-7328.

26. Murray, L. J.; Dinca, M.; Long, J. R., Hydrogen storage in metal-organic frameworks. *Chem. Soc. Rev.* **2009,** *38* (5), 1294-1314.

27. Cao, X.; Tan, C.; Sindoro, M.; Zhang, H., Hybrid micro-/nano-structures derived from metal-organic frameworks: preparation and applications in energy storage and conversion. *Chem. Soc. Rev.* **2017,** *46*, 2660-2677.

28. Horcajada, P.; Serre, C.; Vallet-Regi, M.; Sebban, M.; Taulelle, F.; Ferey, G., Metal-organic frameworks as

efficient materials for drug delivery. *Angew. Chem.-Int. Edit.* **2006,** *45* (36), 5974-5978.

29. Ma, L. Q.; Abney, C.; Lin, W. B., Enantioselective catalysis with homochiral metal-organic frameworks. *Chem. Soc. Rev.* **2009,** *38* (5), 1248-1256.

30. Yu, Y.; Wu, X.-J.; Zhao, M.; Ma, Q.; Chen, J.; Chen, B.; Sindoro, M.; Yang, J.; Han, S.; Lu, Q.; Zhang, H., Anodized Aluminum Oxide Templated Synthesis of Metal–Organic Frameworks Used as Membrane Reactors. *Angew. Chem.-Int. Edit.* **2017,** *56* (2), 578-581.

31. Zhu, H.; Yang, X.; Cranston, E. D.; Zhu, S., Flexible and Porous Nanocellulose Aerogels with High Loadings of Metal–Organic-Framework Particles for Separations Applications. *Adv. Mater.* **2016,** *28* (35), 7652-7657.

32. Chen, Y.; Zhang, S.; Cao, S.; Li, S.; Chen, F.; Yuan, S.; Xu, C.; Zhou, J.; Feng, X.; Ma, X.; Wang, B., Roll-to-Roll Production of Metal-Organic Framework Coatings for Particulate Matter Removal. *Adv. Mater.* **2017,** *29* (15), 1606221.

33. Kreno, L. E.; Leong, K.; Farha, O. K.; Allendorf, M.; Van Duyne, R. P.; Hupp, J. T., Metal-Organic Framework Materials as Chemical Sensors. *Chem. Rev.* **2012,** *112* (2), 1105-1125.

34. Furukawa, H.; Cordova, K. E.; O'Keeffe, M.; Yaghi, O. M., The Chemistry and Applications of Metal-Organic Frameworks. *Science* **2013,** *341* (6149), 1230444.

35. Foo, M. L.; Matsuda, R.; Kitagawa, S., Functional Hybrid Porous Coordination Polymers. *Chem. Mat.* **2014,** *26* (1), 310-322.

36. Lu, G.; Farha, O. K.; Zhang, W. N.; Huo, F. W.; Hupp, J. T., Engineering ZIF-8 Thin Films for Hybrid MOF-Based Devices. *Adv. Mater.* **2012,** *24* (29), 3970-3974.

37. Wang, Q.; Feng, X.; Wang, S.; Song, N.; Chen, Y.; Tong, W.; Han, Y.; Yang, L.; Wang, B., Metal-Organic Framework Templated Synthesis of Copper Azide as the Primary Explosive with Low Electrostatic Sensitivity and Excellent Initiation Ability. *Adv. Mater.* **2016,** *28* (28), 5837-5843.

38. Zhuang, J.; Young, A. P.; Tsung, C.-K., Integration of Biomolecules with Metal–Organic Frameworks. *Small*, 2017,1700880.

39. Doonan, C.; Riccò, R.; Liang, K.; Bradshaw, D.; Falcaro, P., Metal–Organic Frameworks at the Biointerface: Synthetic Strategies and Applications. *Acc. Chem. Res.* **2017,** *50* (6), 1423–1432.

40. Liang, K.; Ricco, R.; Doherty, C. M.; Styles, M. J.; Bell, S.; Kirby, N.; Mudie, S.; Haylock, D.; Hill, A. J.; Doonan, C. J.; Falcaro, P., Biomimetic mineralization of metal-organic frameworks as protective coatings for biomacromolecules. *Nat. Commun.* **2015,** *6*, 7240.

41. Liao, F.-S.; Lo, W.-S.; Hsu, Y.-S.; Wu, C.-C.; Wang, S.-C.; Shieh, F.-K.; Morabito, J. V.; Chou, L.-Y.; Wu, K. C. W.; Tsung, C.-K., Shielding against Unfolding by Embedding Enzymes in Metal–Organic Frameworks via a de Novo Approach. *J. Am. Chem. Soc.* **2017,** *139* (19), 6530-6533.

42. Majewski, M. B.; Howarth, A. J.; Li, P.; Wasielewski, M. R.; Hupp, J. T.; Farha, O. K., Enzyme encapsulation in metal-organic frameworks for applications in catalysis. *CrystEngComm* **2017,** *19*, 4082-4091.

43. Wu, X.; Ge, J.; Yang, C.; Hou, M.; Liu, Z., Facile synthesis of multiple enzyme-containing metal-organic frameworks in a biomolecule-friendly environment. *Chem. Commun* **2015,** *51* (69), 13408-13411.

44. Shieh, F.-K.; Wang, S.-C.; Yen, C.-I.; Wu, C.-C.; Dutta, S.; Chou, L.-Y.; Morabito, J. V.; Hu, P.; Hsu, M.-H.; Wu, K. C. W.; Tsung, C.-K., Imparting Functionality to Biocatalysts via Embedding Enzymes into Nanoporous Materials by a de Novo Approach: Size-Selective Sheltering of Catalase in Metal–Organic Framework Microcrystals. *Journal of the American Chemical Society* **2015,** *137* (13), 4276-4279.

45. Wang, C.; Tadepalli, S.; Luan, J.; Liu, K.-K.; Morrissey, J. J.; Kharasch, E. D.; Naik, R. R.; Singamaneni, S., Metal-Organic Framework as a Protective Coating for Biodiagnostic Chips. *Adv. Mater.* **2016,** *29*, 1604433.

46. Tian, L. M.; Chen, E.; Gandra, N.; Abbas, A.; Singamaneni, S., Gold Nanorods as Plasmonic Nanotransducers: Distance-Dependent Refractive Index Sensitivity. *Langmuir* **2012,** *28* (50), 17435-17442.

47. Chen, H.; Shao, L.; Li, Q.; Wang, J., Gold nanorods and their plasmonic properties. *Chem. Soc. Rev.* **2013,** *42* (7), 2679-2724.

48. Lee, K.-S.; El-Sayed, M. A., Dependence of the Enhanced Optical Scattering Efficiency Relative to That of Absorption for Gold Metal Nanorods on Aspect Ratio, Size, End-Cap Shape, and Medium Refractive Index. *J. Phys. Chem. B* **2005,** *109* (43), 20331-20338.

49. Sau, T. K.; Murphy, C. J., Seeded high yield synthesis of short Au nanorods in aqueous solution. *Langmuir* **2004,** *20* (15), 6414-6420.

50. Tian, L. M.; Morrissey, J. J.; Kattumenu, R.; Gandra, N.; Kharasch, E. D.; Singamaneni, S., Bioplasmonic Paper as a Platform for Detection of Kidney Cancer Biomarkers. *Anal. Chem.* **2012,** *84* (22), 9928-9934.

51. Wang, C.; Hu, R.; Morrissey, J. J.; Kharasch, E. D.; Singamaneni, S., Single Molecule Force Spectroscopy to Compare Natural versus Artificial Antibody–Antigen Interaction. *Small* **2017,** *13* (19), 1604255.

52. Liang, K.; Carbonell, C.; Styles, M. J.; Ricco, R.; Cui, J. W.; Richardson, J. J.; Maspoch, D.; Caruso, F.; Falcaro, P., Biomimetic Replication of Microscopic Metal-Organic Framework Patterns Using Printed Protein Patterns. *Adv. Mater.* **2015,** *27* (45), 7293-7298.

53. Li, S. B.; Dharmarwardana, M.; Welch, R. P.; Ren, Y. X.; Thompson, C. M.; Smaldone, R. A.; Gassensmith, J. J., Template-Directed Synthesis of Porous and Protective Core-Shell Bionanoparticles. *Angew. Chem.-Int. Edit.* **2016,** *55* (36), 10691-10696.

54. Liang, K.; Richardson, J. J.; Cui, J.; Caruso, F.; Doonan, C. J.; Falcaro, P., Metal–Organic Framework Coatings as Cytoprotective Exoskeletons for Living Cells. *Advanced Materials* **2016,** *28* (36), 7910-7914.

55. Zhuang, J.; Kuo, C.-H.; Chou, L.-Y.; Liu, D.-Y.; Weerapana, E.; Tsung, C.-K., Optimized Metal–Organic-Framework Nanospheres for Drug Delivery: Evaluation of Small-Molecule Encapsulation. *Acs Nano*

2014, *8* (3), 2812-2819.

56. Zheng, H.; Zhang, Y.; Liu, L.; Wan, W.; Guo, P.; Nyström, A. M.; Zou, X., One-pot Synthesis of Metal–Organic Frameworks with Encapsulated Target Molecules and Their Applications for Controlled Drug Delivery. *J. Am. Chem. Soc* **2016,** *138* (3), 962-968.

57. Wang, C. Z.; Luan, J. Y.; Tadepalli, S.; Liu, K. K.; Morrissey, J. J.; Kharasch, E. D.; Naik, R. R.; Singamaneni, S., Silk-Encapsulated Plasmonic Biochips with Enhanced Thermal Stability. *ACS Appl. Mater. Interfaces* **2016,** *8* (40), 26493-26500.

58. Kalyanasundaram, K.; Thomas, J. K., The conformational state of surfactants in the solid state and in micellar form. A laser-excited Raman scattering study. *The Journal of Physical Chemistry* **1976,** *80* (13), 1462-1473.

59. Kumari, G.; Jayaramulu, K.; Maji, T. K.; Narayana, C., Temperature Induced Structural Transformations and Gas Adsorption in the Zeolitic Imidazolate Framework ZIF-8: A Raman Study. *J. Phys. Chem. A* **2013,** *117* (43), 11006-11012.

60. Luanwuthi, S.; Krittayavathananon, A.; Srimuk, P.; Sawangphruk, M., In situ synthesis of permselective zeolitic imidazolate framework-8/graphene oxide composites: rotating disk electrode and Langmuir adsorption isotherm. *RSC Adv.* **2015,** *5* (58), 46617-46623.

61. Eslava, S.; Zhang, L.; Esconjauregui, S.; Yang, J.; Vanstreels, K.; Baklanov, M. R.; Saiz, E., Metal-Organic Framework ZIF-8 Films As Low-κ Dielectrics in Microelectronics. *Chem. Mat.* **2013,** *25* (1), 27-33.

62. Park, K. S.; Ni, Z.; Cote, A. P.; Choi, J. Y.; Huang, R. D.; Uribe-Romo, F. J.; Chae, H. K.; O'Keeffe, M.; Yaghi, O. M., Exceptional chemical and thermal stability of zeolitic imidazolate frameworks. *Proc. Natl. Acad. Sci. U. S. A.* **2006,** *103* (27), 10186-10191.

63. Petrova, H.; Juste, J. P.; Pastoriza-Santos, I.; Hartland, G. V.; Liz-Marzan, L. M.; Mulvaney, P., On the temperature stability of gold nanorods: comparison between thermal and ultrafast laser-induced heating. *Phys. Chem. Chem. Phys.* **2006,** *8* (7), 814-821.

64. Yang, X.; Jiang, L.; Jia, Y. G.; Hu, Y.; Xu, Q.; Xu, X.; Huang, H., Counteraction of Trehalose on N,N-Dimethylformamide-Induced Candida rugosa Lipase Denaturation: Spectroscopic Insight and Molecular Dynamic Simulation. *PLoS One* **2016,** *11* (3), e0152275.

65. Mattos, C.; Ringe, D., Proteins in organic solvents. *Curr. Opin. Struct. Biol.* **2001,** *11* (6), 761-764.

66. Cleveland, D. W.; Fischer, S. G.; Kirschner, M. W.; Laemmli, U. K., Peptide mapping by limited proteolysis in sodium dodecyl sulfate and analysis by gel electrophoresis. *J. Biol. Chem.* **1977,** *252* (3), 1102-1106.

67. Rockwood, D. N.; Preda, R. C.; Yucel, T.; Wang, X. Q.; Lovett, M. L.; Kaplan, D. L., Materials fabrication from Bombyx mori silk fibroin. *Nat. Protoc.* **2011,** *6* (10), 1612-1631.

68. Ramachandran, S.; Fu, E.; Lutz, B.; Yager, P., Long-term dry storage of an enzyme-based reagent system for ELISA in point-of-care devices. *Analyst* **2014,** *139* (6), 1456-1462.

69. Jovanović, N.; Bouchard, A.; Hofland, G. W.; Witkamp, G.-J.; Crommelin, D. J. A.; Jiskoot, W., Distinct effects of sucrose and trehalose on protein stability during supercritical fluid drying and freeze-drying. *Eur. J. Pharm. Sci.* **2006,** *27* (4), 336-345.

70. Lee, J. C.; Timasheff, S. N., The stabilization of proteins by sucrose. *J. Biol. Chem.* **1981,** *256* (14), 7193-7201.

71. Zhong, J.; Liu, X. W.; Wei, D. X.; Yan, J.; Wang, P.; Sun, G.; He, D. N., Effect of incubation temperature on the self-assembly of regenerated silk fibroin: A study using AFM. *Int. J. Biol. Macromol.* **2015,** *76*, 195-202.

72. Kononenko, O. K.; Herstein, K. M., Nonaqueous Solvents for Sucrose. *Ind. Eng. Chem. Chem. Eng. Data Series* **1956,** *1* (1), 87-92.

73. Hu, Y. P.; Zhang, Q.; You, R. C.; Wang, L. S.; Li, M. Z., The Relationship between Secondary Structure and Biodegradation Behavior of Silk Fibroin Scaffolds. *Adv. Mater. Sci. Eng.* **2012,** *2012*, 185905.

74. Arai, T.; Freddi, G.; Innocenti, R.; Tsukada, M., Biodegradation of Bombyx mori silk fibroin fibers and films. *J. Appl. Polym. Sci.* **2004,** *91* (4), 2383-2390.

For TOC only

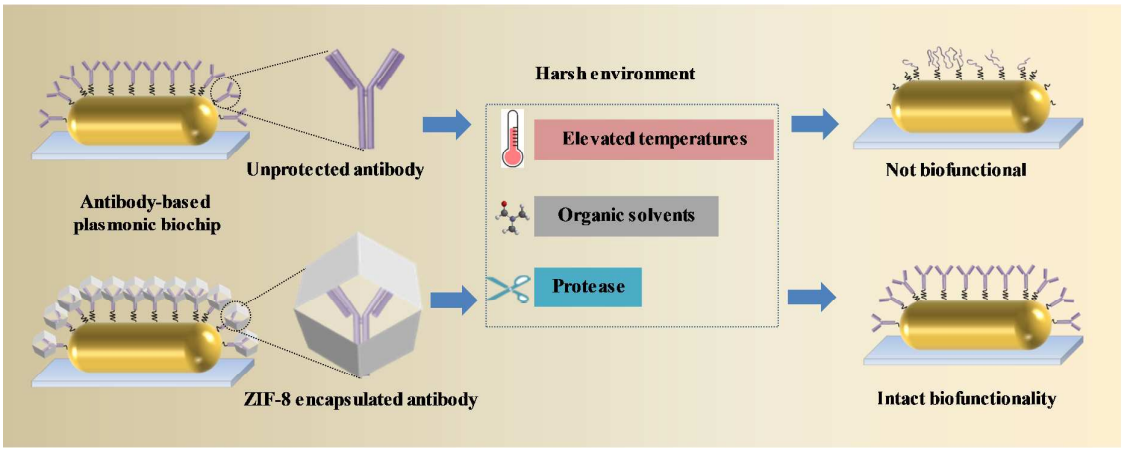
Harsh environment
Elevated temperatures
Organic solvents
Protease
Unprotected antibody
Antibody-based plasmonic biochip
ZIF-8 encapsulated antibody
Not biofunctional
Intact biofunctionality